Published in final edited form as:
Hepatology. 2009 December ; 50(6): 1893–1903. doi:10.1002/hep.23238.

B cell depletion with anti-CD20 ameliorates autoimmune cholangitis but exacerbates colitis in dnTGF-βRII mice

Yuki Moritoki[1,2,*], **Zhe-Xiong Lian**[1,*], **Keith Lindor**[3], **Joseph Tuscano**[4], **Koichi Tsuneyama**[5], **Weici Zhang**[1], **Yoshiyuki Ueno**[2], **Robert Dunn**[6], **Marilyn Kehry**[6], **Ross L. Coppel**[7], **Ian R. Mackay**[8], and **M. Eric Gershwin**[1]

Yuki Moritoki: ymoritoki@ucdavis.edu; Zhe-Xiong Lian: zxlian@ucdavis.edu; Keith Lindor: lindor.keith@mayo.edu; Joseph Tuscano: joseph.tuscano@ucdmc.ucdavis.edu; Koichi Tsuneyama: ktsune@med.u-toyama.ac.jp; Weici Zhang: ddzhang@ucdavis.edu; Yoshiyuki Ueno: yueno@mail.tains.tohoku.ac.jp; Robert Dunn: robert.dunn@biogenidec.com; Marilyn Kehry: marilyn.kehry@biogenidec.com; Ross L. Coppel: ross.coppel@med.monash.edu.au; Ian R. Mackay: ian.mackay@med.monash.edu.au; M. Eric Gershwin: megershwin@ucdavis.edu

[1]Division of Rheumatology, Allergy and Clinical Immunology, University of California, Davis, CA 95616, USA

[2]Division of Gastroenterology, Tohoku University Graduate School of Medicine, Sendai, Miyagi, 980-8575, Japan

[3]Division of Gastroenterology and Hepatology, Mayo Clinic Foundation, Rochester, MN, 55905, USA

[4]Division of Hematology and Oncology, University of California at Davis, Sacramento Medical Center, Sacramento, CA 95817, USA

[5]Diagnostic Pathology, Graduate School of Medicine and Pharmaceutical Science, University of Toyama, Sugitani, Toyama, 930-0194, Japan

[6]Biogen Idec, San Diego, CA 92122, USA

[7]Department of Microbiology, Monash University, Clayton, Victoria, 3800, Australia

[8]Department of Biochemistry and Molecular Biology, Monash University, Clayton, Victoria, 3800, Australia

Abstract

The treatment of primary biliary cirrhosis (PBC) with conventional immunosuppressive drugs has been relatively disappointing and there have been few efforts in defining a role for the newer biological agents useful in rheumatoid arthritis and other systemic autoimmune diseases. In this study we took advantage of dnTGF-βRII mice, a mouse model of autoimmune cholangitis, to address the therapeutic efficacy of B cell depletion using anti-CD20. Mice were treated at either 4–6 weeks of age or beginning at 20–22 weeks of age with IP injections of anti-CD20 every two weeks. We quantitated B cell levels in all mice as well as antimitochondrial antibodies (AMA),

Correspondence to: M. Eric Gershwin, M.D., Division of Rheumatology, Allergy and Clinical Immunology, University of California at Davis School of Medicine, 451 Health Sciences Drive, Suite 6510, Davis, CA 95616; Telephone: 530-752-2884; Fax: 530-752-4669; megershwin@ucdavis.edu.
*These authors contributed equally to this work.

No conflicts of interest exist

serum and hepatic levels of pro-inflammatory cytokines and histopathology of liver and colon. In mice whose treatment was initiated at 4–6 weeks of age, anti-CD20 therapy demonstrated a significant lower incidence of liver inflammation associated with reduced numbers of activated hepatic $CD8^+$ T cells. However, colon inflammation was exacerbated. In contrast, in mice treated at 20–22 weeks of age, anti-CD20 therapy had relatively little effect on either liver or colon disease. As expected all treated animals had reduced levels of B cells, absence of AMA, and increased levels in sera of TNFα, IL-6 and CCL2 (MCP-1). These data suggest potential usage of anti-CD20 in early PBC resistant to other modalities, but raise the cautionary note regarding the use of anti-CD20 in IBD.

Keywords

Autoimmune cholangitis; Primary biliary cirrhosis; B cells

The destruction of biliary epithelial cells (BEC) in primary biliary cirrhosis (PBC) is primarily attributed to autoreactive T cells (1–8). In contrast, the contribution of B cells to PBC immunopathology remains unclear (9), despite the nearly universal occurrence in serum of autoantibodies to the pyruvate dehydrogenase E subunit (PDC-E2, anti-mitochondrial antibodies [AMA]), the major auto-antigen in human PBC. Nonetheless, a role for B cells has been suggested. For example, the inflammatory liver infiltrates include foci of B cells (10). Autoantibodies to the E2 subunit of the PDC enzymes inhibit catalytic activity (11, 12), which is reasoned to facilitate IgA-AMA transcytosis through the BEC in the form of dimeric IgA-AMA complexes leading to the induction of apoptosis of these cells (13). Moreover, autoantibodies to PDC-E2 markedly enhanced the cross presentation and generation of PDC-E2-specific cytotoxic T cell responses in the presence of PDC-E2-pulsed antigen presenting cells (14). However, neither the presence nor levels of AMA following orthotopic liver transplantation for PBC correlate with the recurrence of PBC (15). Thus, notwithstanding the evidence for a profound loss of both B- (and T-) cell tolerance to the autoantigenic epitope(s) of PDC-E2, the degree to which B cells or autoantibodies are involved as effector elements in the pathogenesis of BEC damage in PBC remains unresolved.

In one of our mouse models of PBC, the TGF-β receptor II dominant negative (dnTGF-βRII) mice, there is a readily detectable inflammatory lymphocytic infiltrate in the liver (16) that closely simulates that seen in chronic non-suppurative destructive cholangitis of human PBC. In this model, the expression of dnTGF-βRII receptor is restricted to select cell lineages including the $CD4^+$, $CD8^+$, and the CD1d-restricted natural killer T (NKT) cell lineages (16). In efforts to address the role of B cells we treated 4 to 6 week and 20 to 22 week old dnTGF-βRII mice with anti-CD20 monoclonal antibody (mAb). Whereas the PBC-like disease is markedly attenuated in young mice, the colitis was exacerbated. The same therapy of older mice showed no such difference in the severity of either cholangitis and/or colitis. Although anti-CD20 therapy has potential efficacy in PBC, our data argue that effectiveness may be restricted to early stage patients and further that there is a potential for exacerbation of any underlying IBD.

Methods

dnTGF-βRII mice

dnTGF-βRII mice were bred onto a C57BL/6 (B6) strain background (The Jackson Laboratory, Bar Harbor, Maine) at the animal facilities of the University of California at Davis (16, 17). Male heterozygous dnTGFβ-RII mice were bred with female B6 mice to obtain female heterozygous dnTGFβ-RII mice, which were genotyped to confirm the dnTGFβ-RII gene in their genomic DNA by the detection of the CD4 promoter at the age of 3–4 weeks (17). All mice were fed a sterile rodent *Helicobacter* Medicated Dosing System (three-drug combination) diet (Bio-Serv, Frenchtown, NJ) and maintained in individually ventilated cages under specific pathogen-free conditions.

Immunotherapy

Anti-mouse CD20 IgG2a and an isotype-matched control mAb utilized herein have been previously described (18). An optimal dose of sterile anti-mouse CD20 IgG2a or isotype-matched control mAbs (250μg/250 μl in PBS) were injected intraperitoneally into dnTGFβ-RII mice using a 27G needle every 2 weeks from 4–6, or 20–22 weeks of age. Peripheral blood samples from individual mice were obtained from the retro-orbital vascular plexus before initial treatment and then at two week intervals. Sera were stored at −70°C until use. The Animal Care and Use Committee in University of California Davis approved all studies.

Humoral immunity

Serum levels of IgG, IgA, and IgM were measured using a mouse Ig isotype quantitative ELISA kit (BETHYL, Montgomery, TX). Known standards were used throughout. Serum levels of anti-PDC-E2 were quantified using an ELISA. Briefly, 96-well ELISA –plates were coated with purified recombinant (r) PDC-E2 at 10 μg/mL in carbonate buffer (pH 9.6) at 4°C overnight, washed 5 times with PBS containing 0.05% Tween-20 (Fisher Biotech, Fair Lawn, NJ) (PBS-T), and blocked with 3% skim milk in PBS for 30 minutes. 100 μL of the sera to be tested diluted 1:200 were added to individual wells of this microtiter plate for 1 hour at room temperature (RT) and the plates re-washed. 100 μL of horseradish peroxidase (HRP)-conjugated anti-mouse immunoglobulin (G+A+M) (H+L) (1:2,000) (Zymed, San Francisco, CA) was added to each well for 1 hour at RT, and the microtiter wells were re-washed. Immunoreactivity was detected by measuring the optical density (OD) at 450 nm after exposure for 15 minutes to 100 μL of TMB peroxidase substrate (KPL, Gaithersburg, MD). Previously calibrated positive and negative standards were included with each assay.

Flow Cytometry

Peripheral blood mononuclear cells (PBMC) were isolated from heparinized murine blood using Accupaque (Accurate Chemical & Scientific Company, Westbury, CT) to confirm the levels of B cells. Cells were pre-incubated with anti-mouse FcR blocking reagent and then incubated at 4°C with a pre-determined optimum concentration of PE-Cy5.5 conjugated anti-CD4 (BioLegend), PE-conj. anti-mouse IgM (Caltag), and FITC conjugated anti-CD19 (BioLegend). In addition, mononuclear cells were isolated from liver and spleen suspensions as previously described (16). An aliquot of these cells was pre-incubated with anti-mouse

FcR blocking reagent and then incubated at 4°C with a combination of fluorochrome-conjugated Abs, including PE conjugated anti-CD4 (Pharmingen, San Diego, CA), PE-Cy5 conjugated anti-CD8a (eBioscience), APC-Cy7 conjugated anti-CD3 (BD biosciences, San Jose, CA), APC conjugated anti-NK1.1 (BioLegend), FITC conjugated anti-CD44 (BioLegend), and PE-Cy5 conjugated anti-CD19 (BioLegend). Multi-color flow analyses were performed using a FACScan flow cytometer (BD Immunocytometry Systems, San Jose, CA) upgraded by Cytec Development (Fremont, CA) to allow for 5-color analysis. Acquired data were analyzed with CELLQUEST Software (BD Biosciences).

Liver, Spleen, Ileum, and Colon Tissue Preparations

Portions of the liver, spleen, terminal ileum, and colon were excised and immediately fixed with 10% buffered formalin solution for 2 days at RT. Paraffin-embedded tissue sections were then cut into 4-μm slices for routine hematoxylin (DakoCytomation, Carpinteria, CA) and eosin (American Master Tech Scientific, Lodi, CA) (H&E) staining. Scoring of liver inflammation was performed on coded H &E stained sections of liver using a set of 3 indices by a “blinded” pathologist (KT); indices included degrees of portal inflammation, parenchymal inflammation and bile duct damage were scored as 0 = nil, 1= minimal, 2= mild, 3= moderate and 4 = severe pathology. Scoring of ileum and colon inflammation was based on four indices that included degrees of mucosal erosion, inflammation, epithelial change, and presence of crypt abscesses.

Cytokine Analysis

The inflammatory cytokines, TNF-α, IL-6, IL-10, IL-12p70, and IFN-γ, and the chemokine CCL2 (MCP-1) were quantitated in sera and in preparations of total liver protein using a mouse cytokine cytometric bead array (BD Biosciences). To extract total liver protein, 100–200 mg of frozen liver tissue were homogenized in TNE buffer (1% NP 40, 10 mM Tris-HCl pH 7.5, 150 mM NaCl, 1 mM EDTA) containing a cocktail of protease and phosphatase inhibitors (Roche, Indianapolis, IN), as previously described (19). The suspension was centrifuged at 7200 g for 20 min at 4 °C and stored at −80 °C. The protein concentration was measured using the BCA kit (Pierce Biotechnology, Rockford, IL). Fifty μg of this protein preparation was utilized for the quantitation of cytokines.

Immunohistochemistry

Abs against CK22 (monoclonal mouse anti-human cytokeratin (cross reactive with murine cytokeratin), GeneTex, San Antonio, TX), TNF-α (rabbit anti-mouse TNF-α, 1:20, Monosan, Uden, The Netherlands), IL-6 (IL-6 goat-polyclonal anti-mouse IL-6, 1:100, R&D Systems, Minneapolis, MN), and MCP-1 (goat-polyclonal anti-MCP-1, 1:100, Santa Cruz, CA), were used for immunohistochemical staining of liver and colon sections as previously described (20). Tissue sections were cut at 4μm from tissue blocks and placed on slides. After de-paraffinization, sections were soaked in target retrieval buffered saline (TRS, pH 6.1, Dako Cytomation, Carpinteria, CA) in a non-metal containing plastic-made pressure cooker and irradiated in a microwave oven for 10 minutes (maximum 500W). After irradiation, sections were rinsed under running water for 2 minutes, soaked in 3% H_2O_2 methanol solution for 5 minutes, and then soaked in 5%BSA for 1 minute. Primary antibodies were diluted to a previously determined optimal concentration in PBS containing

5% BSA. The diluted antibodies were applied to the tissue sections in a moist chamber and irradiated intermittently for 10 minutes (250W, 4 seconds-on, 3 seconds-off). After 3 washes with Tris-buffered saline containing 1% Tween (TBS-T) for 1 minute, peroxidase-conjugated Envision kit for rabbit (Envision-PO, Envision System, Dako Cytomation), Histofine-PO for goat and mouse (Nichirei, Tokyo, Japan) were applied on the appropriate specimens in the moist chamber. Irradiation was then performed intermittently for 10 minutes, as described above. After washing x5 with TBS-T, the sections were immersed in DAB solution (Sigma-Aldrich) with H_2O_2 and counterstained with Hematoxylin (Dako Cytomation) and mounted under coverslips.

Presentation of Data and Statistical Analysis

Values were expressed graphically as the mean ± standard error of the mean (SEM). Differences were tested for significance by a two-tailed unpaired Mann-Whitney test. The frequency of portal inflammation and bile duct damage were evaluated using Fisher's exact test. Values having $p < 0.05$ were considered statistically significant.

Results

Anti-CD20 treatment depletes peripheral B cells, AMA and sera immunoglobulin in dnTGF-βRII mice. We monitored the depletion of peripheral $CD19^+$ B cells following the intraperitoneal administration of anti-CD20 mAb. As noted in Figure 1A and B, the frequency of $CD19^+$ B cells decreased to nearly undetectable levels at 2 weeks after the initial treatment at 4 to 6 week and 20 to 22 week old of dnTGF-βRII mice. Sera from dnTGF-βRII mice contained significant levels of anti-rPDC-E2 prior to treatment with the anti-CD20 antibody. However these titers decreased markedly following treatment (Figure 2). This decrease in rPDC-E2 reactivity was accompanied by a significant reduction of serum IgM, IgA and IgG (Figure 2).

Anti-CD20 treatment ameliorates PBC-like liver disease in young dnTGF-βRII mice

Liver sections from anti-CD20 treated dnTGF-βRII mice demonstrated a marked diminution of liver inflammation and bile duct damage as determined by the use of anti-CK22 to highlight hepatocytes and cholangiocytes (Figure 3A). In addition, hepatic inflammatory cell infiltrates were seldom observed in comparison to dnTGF-βRII mice administered the control mAb. Thus, anti-CD20 treatment ameliorated liver inflammation and bile duct damage in dnTGF-βRII mice (Figure 3B, C). The degrees of portal tract and hepatic parenchymal inflammation plotted individually are shown in figures 3D. Of note, the fortnightly treatment regimen of the ant-CD20 mAb described above did not induce any inflammation in the liver or colon of control B6 littermates (data not shown).

Anti-CD20 has no effect on older dnTGFβ-RII mice

The data obtained on tissues from the older (20–22 to 36–38 week old) dnTGF-βRII mice treated with the anti-CD20 mAb were rather different. Therapy induced neither improvement of liver inflammation nor exacerbation of colitis. Although in some of the anti-CD20 treated mice, inflammation in the liver was milder and in the colon more severe compared with controls (Figure 3E–H and 5C,D). Anti-CD20 treatment efficiently depleted

B cells in peripheral blood, liver and spleen (Figure 1B and 4), and reduced serum reactivity to rPDC-E2 (Figure 2).

B cell depletion by anti-CD20 reduces the level of $CD8^+$ T cell infiltrates in the liver of young dnTGF-βRII mice

Flow cytometric analysis demonstrated that anti-CD20 treatment efficiently depleted B cells in the liver and spleen. Of interest was the finding that while anti-CD20 treatment of dnTGF-βRII mice markedly reduced the numbers of $CD8^+$ T cells and their activated phenotypes in the liver, the frequency of $CD8^+$ T cells were only slightly reduced in spleen and similar to mice treated with the control mAb. On the other hand, the number of $CD4^+$ T cells was comparable in liver of the anti-CD20 treated dnTGF-βRII mice and control mAb treatment (Figure 4). Anti-CD20 treatment efficiently depleted splenic B cells, however, total and activated cell numbers of $CD4^+$ and $CD8^+$ T lymphocytes in spleen did not differ significantly after anti-CD20 treatment.

Colon inflammation in young dnTGF-βRII mice exacerbated by anti-CD20 treatment

Histologically, the colon of the anti-CD20 treated dnTGF-βRII mice demonstrated severe inflammation compared with normal B-cell-intact mice (Figure 5A). The degree of colon inflammation differed significantly for the two groups (Figure 5B).

Cytokine profiles in serum, liver, and colon

The levels of inflammatory cytokines in dnTGF-βRII mice were modulated by anti-CD20 treatment. Serum levels of inflammatory cytokines, IL-6 and TNF-α, and MCP-1 were greater after anti-CD20 treatment compared to those of similarly-treated control mAb treated mice (Figure 6A–C), whereas levels of IFN-γ, IL-12p70, and IL-10 were below the levels of detection in any of the serum samples (data not shown). While the levels of IL-6 was the only pro-inflammatory cytokine that was significantly increased in extracted total hepatic proteins from the anti-CD20 treated mice as compared with mice treated with the control mAb (Figure 6A), the levels of IL-12p70, IL-10 and MCP-1 were similar in the anti-CD20 as compared with the mice treated with the control mAb (Figure 6B and data not shown). TNF-α and IFN-γ were below levels of detection in the liver protein extract of both groups of mice (Figure 6C and data not shown). The cytokine profile in the liver and colon was also investigated immunohistochemically. IL-6 was readily detected on hepatocytes and cholangiocytes in tissue sections from both the anti-CD20 treated mice and controls (Figure 6D). In addition, IL-6 positive mononuclear cells were present among colonic cell infiltrates in both groups of mice, and the cytoplasm of epithelial cells on the mucosal surface and within crypt lumens were also positive for IL-6 in the anti-CD20 treated mice. MCP-1 was also readily detectable in hepatocytes and cholangiocytes, and strongly so in Kupffer cells and portal infiltrating lymphocytes. The degree of staining for MCP-1 in infiltrating mononuclear cells was increased in colon tissues of anti-CD20 treated mice compared to controls (Figure 6E). While TNF-α positive cells were observed in the colon, but not in liver tissues of anti-CD20 treated mice, TNF-α positive cells were lacking in both liver and colon tissues from mice treated with the control mAb (Figure 6F). IFN-γ was undetectable in both liver and colon tissues irrespective of treatment (data not shown).

Discussion

We demonstrate herein that therapeutic deletion of B lymphocytes in the dnTGF-βRII mouse model of PBC using an anti-CD20 Ab ameliorated liver inflammation compared to B cell competent dnTGF-βRII mice. Further, liver cell infiltrates from B cell depleted dnTGF-βRII mice contained reduced populations of $CD8^+$ T cells and their activated phenotypes, and increased serum levels of TNF-α, IL-6 and CCL2 (MCP-1) compared to B cell sufficient dnTGF-βRII mice. Thus not only do B cells promote the development of PBC-like liver disease in younger dnTGF-βRII mice, but also freshly primed B cells possibly including those with specificity for PDC-E2 may enhance progression of inflammatory liver responses.

Data from our recent report suggests the existence of B cell subsets with a regulatory function i.e., Breg cells in dnTGF-βRII mice (21) as has been reported for several other autoimmne diseases (22, 23). The dnTGF-βRII mice display features of colitis, in addition to cholangitis (17), and since genetic B-cell depletion in dnTGF-βRII mice augments inflammation in the colon as well as the liver, Bregs are thought to be primarily functional from initiation to progression of both colitis and autoimmune cholangitis in this genetically modified strain. However, others recently demonstrated the existence of B cell subsets with opposing activities, i.e. promoting or suppressing disease progression. In mouse EAE the contributions of B cells are dependent on time in the course of disease initiation and progression (24).

To examine whether the primary function of B cells differs in the course of disease progression in dnTGF-βRII mice, we studied therapeutic B cell depletion of dnTGF-βRII mice at younger and older ages in comparison to B cell competent dnTGF-βRII mice. To deplete B cells sufficiently, we administered anti-CD20 mAb intraperitoneally (25). Peripheral B cells were well depleted in the two groups, two weeks after initial treatment using anti-CD20 (Figure 1).

As described above, while B cell depletion from the 4–6 week old young dnTGF-βRII mice demonstrated a marked reduction of liver disease (Figure 3), such reduction of inflammation was not noted in liver tissues from the 20–22 week old aged mice (Figure 3). In fact, data from the flow cytometric analysis indicate that the absolute numbers of $CD8^+$ T cells and their activated phenotype of CD44-expressing $CD8^+$ T cells were significantly diminished in the livers of B cell depleted young, but not old, dnTGF-βRII mice (Figure 4). Given that $CD8^+$ T cells are the primary contributors to autoimmune cholangitis in our adoptive transfer model (21, 26), and the observed reduction in the $CD8^+$ T cell population in the liver herein, we can suggest that in young mice B cells mediate the hepatic infiltration of $CD8^+$ T cells from the extra-hepatic lymphoid organs.

In addition, B cell depletion in young dnTGF-βRII mice may suppress development of PDC-E2 primed $CD8^+$ T cells due to the depletion of Ig against PDC-E2, i.e.AMA, which was more efficiently depleted in the sera from the young anti-CD20 treated mice (Figure 2). Antigen presenting cells may ligate PDC-E2-Ig immune complexes on their Fc receptors and cross-prime $CD8^+$ T cells into activated PDC-E2 reactive phenotypes (14). Insufficient

depletion of Ig specific for PDC-E2 may allow the development of autoreactive T cells in older mice. On the other hand, data herein demonstrate no improvement of colonic disease in mice of any age by anti-CD20 treatment (Figure 5) which is compatible to anti-CD20 treatment in human IBD (26). Thus, these data suggest that the role of B cells in biliary ductular and colonic inflammatory diseases are distinguishable in young dnTGF-βRII mice.

Since we previously found that serum concentrations of TNF-α and IL-6 were significantly greater in Igμ$^{-/-}$dnTGF-βRII compared to dnTGF-βRII control littermates (21), we studied an extensive profile of inflammatory cytokines in anti-CD20 treated mice. In the current investigation, serum levels of both of these cytokines, as well as the chemokine CCL2 (MCP-1), were increased upon B cell depletion. In addition, we examined hepatic protein levels of inflammatory mediators. While there was a marked increase in the level of IL-6 protein in liver of anti-CD20 treated mice, the levels of CCL2 (MCP-1) were comparable. TNF-α was lower than the detectable range in this assay. However, since there was discrepancy between serum and hepatic levels of inflammatory cytokines, and to explain the ameliorated liver inflammation, we further investigated cytokines profiles in liver and colon immunohistochemically. In contrast to the increased levels of TNF-α in sera, TNF-α was undetectable in the liver. However, some of the mononuclear cells were positive for TNF-α in the colon of anti-CD20 treated mice (Figure 6F). Thus, B cells are likely to regulate TNF-α producing cells in colonic inflammation, which are unlikely to mediate hepatic inflammation in this strain. In fact, anti-TNF-α therapy has been documented to dramatically improve outcome of human IBD (27). On the other hand, IL-6 was observed in hepatocytes and cholangiocytes in liver and colon tissues from the anti-CD20 treated mice whereas IL-6 was positive in colon tissues of control mice (Figure 6D). These data suggest that IL-6 is up-regulated by anti-CD20 treatment of mice but that such increased IL-6 levels play opposing roles in liver and colon inflammation, i.e. participation in the amelioration of the PBC-like liver disease but exacerbation of colitis, as reported in ConA-hepatitis and intestinal inflammation by others (28, 29). Improved liver inflammation is likely to reflect a milder infiltration of CD8$^+$ T cells by B cell depletion, borne out by flow cytometric analysis showing that the number of CD44-expressing activated CD8$^+$ T cells was significantly decreased in the livers of B cell depleted dnTGF-βRII mice. Thus, the amelioration of liver disease in B cell depleted mice indicates that the presumed pro-inflammatory function of hepatic B cells is at least partially mediated by the suppression of IL-6 by activated CD8$^+$ T cells.

Similar to our recent report, we failed to detect IL-10 in the serum of anti-CD20 treated dnTGF-βRII mice and controls (data not shown) (21). Also, hepatic IL-10 protein levels were comparable for anti-CD20 treated mice and controls (data not shown). Since anti-CD20 treated mice demonstrated ameliorated liver inflammation compared to controls, it is unlikely that hepatic B cell-derived IL-10 plays an essential immunoregulatory role in autoimmune cholangitis in this genetically modified strain.

PBC patients frequently demonstrate sicca syndromes (30), and PBC sera have been shown to react with apoptotic blebs and bodies of epithelia of human intrahepatic bile duct as well as salivary gland, but not other cells (31). Immune complexes binding to apoptotic bodies may enhance priming of bile duct and salivary gland reactive CD8$^+$ T cells through antigen

presentation (14). Indications for anti-CD20 treatment are expanding in human autoimmune diseases. Rituximab (an anti-human CD20 monoclonal antibody) therapy has shown promise for the treatment of Sjogren's syndrome (32). Also, similar to our present data in a murine model of human PBC model, anti-CD20 treatment ameliorated adenitis of submandibular and lacrimal glands in Id3 knock out mice, a model of primary Sjögren's syndrome (33). In one pilot study, in which Rituximab was used for the therapy of PBC patients who were refractory to ursodeoxycholic acid (UDCA), there was reduction of serum ALP, and AMA and IgM levels, accompanied by reduced pruritus and fatigue (34).

Again, we demonstrated in the present study that anti-CD20 treatment ameliorated PBC-like liver disease, accompanied with a reduction in hepatic $CD8^+$ T cells in young dnTGF-βRII mice. Since PDC-E2 reactive $CD8^+$ T cells have been considered as main contributors to bile duct damage in human PBC (14), therapeutic B cell depletion may be efficacious in regulating such damage by suppressing expansion of PDC-E2 reactive $CD8^+$ T cells. Clearly, the mechanism of action of anti-CD20 is complex and our data and that of others argues that it extends far beyond simple B cell depletion; such observations have been made in several models of autoimmunity as well as in clinical studies of treated patients (35–42). Our approach to address the mechanism in more detail will be to continue adoptive transfer studies, similar to our previous published work (21). Our present data provide a rationale for therapeutic B cell depletion using Rituximab in human PBC although the timing of therapeutic B cell depletion may be critically dependent on use in the earlier stages of the disease.

Acknowledgments

Grant Support: This work was supported by National Institute of Health grants (DK39588 and DK074768, M.E.G.; DK077961, Z.X.L.), UCD Center for Health and Nutrition Research Pilot Grant (Z.X.L.).

We would like to thank Dr. Katsunori Yoshida and Dr. Guo-Xiang Yang for performing ELISA and technical support in this experiment. Also, we appreciate the helpful support of Ms. Nikki Phipps in preparing this manuscript.

Abbreviations

AMA	anti-mitochondrial autoantibodies
Bregs	B regulatory cells
dnTGF-β RII mice	TGF-β receptor II dominant negative mice
TGF-β	transforming growth factor-β

References

1. Gershwin ME, Ansari AA, Mackay IR, Nakanuma Y, Nishio A, Rowley MJ, et al. Primary biliary cirrhosis: an orchestrated immune response against epithelial cells. Immunol Rev. 2000; 174:210–225. [PubMed: 10807518]
2. Kamihira T, Shimoda S, Harada K, Kawano A, Handa M, Baba E, et al. Distinct costimulation dependent and independent autoreactive T-cell clones in primary biliary cirrhosis. Gastroenterology. 2003; 125:1379–1387. [PubMed: 14598254]

3. Kamihira T, Shimoda S, Nakamura M, Yokoyama T, Takii Y, Kawano A, et al. Biliary epithelial cells regulate autoreactive T cells: implications for biliary-specific diseases. Hepatology. 2005; 41:151–159. [PubMed: 15619239]
4. Kaplan MM, Gershwin ME. Medical progress: Primary biliary cirrhosis. N Engl J Med. 2005; 353:1261–1273. [PubMed: 16177252]
5. Shigematsu H, Shimoda S, Nakamura M, Matsushita S, Nishimura Y, Sakamoto N, et al. Fine specificity of T cells reactive to human PDC-E2 163–176 peptide, the immunodominant autoantigen in primary biliary cirrhosis: implications for molecular mimicry and cross-recognition among mitochondrial autoantigens. Hepatology. 2000; 32:901–909. [PubMed: 11050037]
6. Shimoda S, Ishikawa F, Kamihira T, Komori A, Niiro H, Baba E, et al. Autoreactive T-cell responses in primary biliary cirrhosis are proinflammatory whereas those of controls are regulatory. Gastroenterology. 2006; 131:606–618. [PubMed: 16890612]
7. Shimoda S, Nakamura M, Ishibashi H, Kawano A, Kamihira T, Sakamoto N, et al. Molecular mimicry of mitochondrial and nuclear autoantigens in primary biliary cirrhosis. Gastroenterology. 2003; 124:1915–1925. [PubMed: 12806624]
8. Shimoda S, Nakamura M, Shigematsu H, Tanimoto H, Gushima T, Gershwin ME, et al. Mimicry peptides of human PDC-E2 163–176 peptide, the immunodominant T-cell epitope of primary biliary cirrhosis. Hepatology. 2000; 31:1212–1216. [PubMed: 10827144]
9. He X-S, Ansari AA, Ridgway WM, Coppel RL, Gershwin ME. New insights to the immunopathology and autoimmune responses in primary biliary cirrhosis. Cellular Immunology. 2006; 239:1–13. [PubMed: 16765923]
10. Nakanuma Y. Distribution of B lymphocytes in nonsuppurative cholangitis in primary biliary cirrhosis. Hepatology. 1993; 18:570–575. [PubMed: 8359797]
11. Fregeau DR, Prindiville T, Coppel RL, Kaplan M, Dickson ER, Gershwin ME. Inhibition of alpha-ketoglutarate dehydrogenase activity by a distinct population of autoantibodies recognizing dihydrolipoamide succinyltransferase in primary biliary cirrhosis. Hepatology. 1990; 11:975–981. [PubMed: 2365294]
12. Fregeau DR, Roche TE, Davis PA, Coppel R, Gershwin ME. Primary biliary cirrhosis. Inhibition of pyruvate dehydrogenase complex activity by autoantibodies specific for E1 alpha, a non-lipoic acid containing mitochondrial enzyme. J Immunol. 1990; 144:1671–1676. [PubMed: 2106552]
13. Matsumura S, Van De Water J, Leung P, Odin JA, Yamamoto K, Gores GJ, et al. Caspase induction by IgA antimitochondrial antibody: IgA-mediated biliary injury in primary biliary cirrhosis. Hepatology. 2004; 39:1415–1422. [PubMed: 15122771]
14. Kita H, Lian ZX, Van de Water J, He XS, Matsumura S, Kaplan M, et al. Identification of HLA-A2-restricted CD8(+) cytotoxic T cell responses in primary biliary cirrhosis: T cell activation is augmented by immune complexes cross-presented by dendritic cells. J Exp Med. 2002; 195:113–123. [PubMed: 11781370]
15. Neuberger J. Liver transplantation for primary biliary cirrhosis. Autoimmunity Reviews. 2003; 2:1–7. [PubMed: 12848968]
16. Oertelt S, Lian Z-X, Cheng C-M, Chuang Y-H, Padgett KA, He X-S, et al. Anti-mitochondrial antibodies and primary biliary cirrhosis in TGF-beta receptor II dominant-negative mice. Journal of Immunology. 2006; 177:1655–1660.
17. Gorelik L, Flavell RA. Abrogation of TGFb signaling in T cells leads to spontaneous T cell differentiation and autoimmune disease. Immunity. 2000; 12:171–181. [PubMed: 10714683]
18. Hamel K, Doodes P, Cao Y, Wang Y, Martinson J, Dunn R, et al. Suppression of proteoglycan-induced arthritis by anti-CD20 B Cell depletion therapy is mediated by reduction in autoantibodies and CD4+ T cell reactivity. J Immunol. 2008; 180:4994–5003. [PubMed: 18354225]
19. Zhang W, Sharma R, Ju ST, He XS, Tao Y, Tsuneyama K, et al. Deficiency in regulatory T cells results in development of antimitochondrial antibodies and autoimmune cholangitis. Hepatology. 2008; 49:545–552. [PubMed: 19065675]
20. Kumada T, Tsuneyama K, Hatta H, Ishizawa S, Takano Y. Improved 1-h rapid immunostaining method using intermittent microwave irradiation: practicability based on 5 years application in Toyama Medical and Pharmaceutical University Hospital. Mod Pathol. 2004; 17:1141–1149. [PubMed: 15167936]

21. Moritoki Y, Zhang W, Tsuneyama K, Yoshida K, Wakabayashi K, Yang GX, et al. B Cells Suppress the Inflammatory Response in a Mouse Model of Primary Biliary Cirrhosis. Gastroenterology. 2009; 136:1037–1047. [PubMed: 19118554]
22. Bouaziz JD, Yanaba K, Tedder TF. Regulatory B cells as inhibitors of immune responses and inflammation. Immunol Rev. 2008; 224:201–214. [PubMed: 18759928]
23. Mizoguchi A, Bhan AK. A case for regulatory B cells. Journal of Immunology. 2006; 176:705–710.
24. Matsushita T, Yanaba K, Bouaziz JD, Fujimoto M, Tedder TF. Regulatory B cells inhibit EAE initiation in mice while other B cells promote disease progression. J Clin Invest. 2008; 118:3420–3430. [PubMed: 18802481]
25. Hamaguchi Y, Uchida J, Cain DW, Venturi GM, Poe JC, Haas KM, et al. The peritoneal cavity provides a protective niche for B1 and conventional B lymphocytes during anti-CD20 immunotherapy in mice. J Immunol. 2005; 174:4389–4399. [PubMed: 15778404]
26. Papadakis KA, Rosenbloom B, Targan SR. Anti-CD2O chimeric monoclonal antibody (rituximab) treatment of immune-mediated thrombocytopenia associated with Crohn's disease. Gastroenterology. 2003; 124:583. [PubMed: 12557172]
27. Kozuch PL, Hanauer SB. Treatment of inflammatory bowel disease: a review of medical therapy. World J Gastroenterol. 2008; 14:354–377. [PubMed: 18200659]
28. Atreya R, Neurath MF. Signaling molecules: the pathogenic role of the IL-6/STAT-3 trans signaling pathway in intestinal inflammation and in colonic cancer. Curr Drug Targets. 2008; 9:369–374. [PubMed: 18473764]
29. Sun R, Tian Z, Kulkarni S, Gao B. IL-6 prevents T cell-mediated hepatitis via inhibition of NKT cells in CD4+ T cell- and STAT3-dependent manners. J Immunol. 2004; 172:5648–5655. [PubMed: 15100309]
30. Leuschner U. Primary biliary cirrhosis--presentation and diagnosis. Clin Liver Dis. 2003; 7:741–758. [PubMed: 14594129]
31. Lleo A, Selmi C, Invernizzi P, Podda M, Coppel RL, Mackay IR, et al. Apotopes and the biliary specificity of primary biliary cirrhosis. Hepatology. 2009; 49:871–879. [PubMed: 19185000]
32. Isaksen K, Jonsson R, Omdal R. Anti-CD20 treatment in primary Sjogren's syndrome. Scand J Immunol. 2008; 68:554–564. [PubMed: 19000095]
33. Hayakawa I, Tedder TF, Zhuang Y. B-lymphocyte depletion ameliorates Sjogren's syndrome in Id3 knockout mice. Immunology. 2007; 122:73–79. [PubMed: 17472721]
34. Myers R, Shaheen A, Swain M, Lee S, Cole S, Coffey-Williamson S, et al. Rituximab for primary biliary cirrhosis (PBC) refractory to ursodeoxycholic acid (UDCA). Hepatology. 2007; 46:550A.
35. Marino E, Grey ST. A new role for an old player: do B cells unleash the self-reactive CD8+ T cell storm necessary for the development of type 1 diabetes? J Autoimmun. 2008; 31:301–305. [PubMed: 18809297]
36. Shimoda S, Miyakawa H, Nakamura M, Ishibashi H, Kikuchi K, Kita H, et al. CD4 T-cell autoreactivity to the mitochondrial autoantigen PDC-E2 in AMA-negative primary biliary cirrhosis. J Autoimmun. 2008; 31:110–115. [PubMed: 18644699]
37. Lyons JA, Ramsbottom MJ, Mikesell RJ, Cross AH. B cells limit epitope spreading and reduce severity of EAE induced with PLP peptide in BALB/c mice. J Autoimmun. 2008; 31:149–155. [PubMed: 18539432]
38. Vital EM, Emery P. The development of targeted therapies in rheumatoid arthritis. J Autoimmun. 2008; 31:219–227. [PubMed: 18501558]
39. Poletaev AB, Stepanyuk VL, Gershwin ME. Integrating immunity: the immunculus and self-reactivity. J Autoimmun. 2008; 30:68–73. [PubMed: 18191542]
40. Rowley B, Tang L, Shiniton S, Hayakawa K, Hardy RR. Autoreactive B-1 B cells: constraints on natural autoantibody B cell antigen receptors. J Autoimmun. 2007; 29:236–245. [PubMed: 17889506]
41. Fekete A, Soos L, Szekanecz Z, Szabo Z, Szodoray P, Barath S, et al. Disturbances in B- and T-cell homeostasis in rheumatoid arthritis: suggested relationships with antigen-driven immune responses. J Autoimmun. 2007; 29:154–163. [PubMed: 17826949]

42. Youinou P. B cell conducts the lymphocyte orchestra. J Autoimmun. 2007; 28:143–151. [PubMed: 17363215]

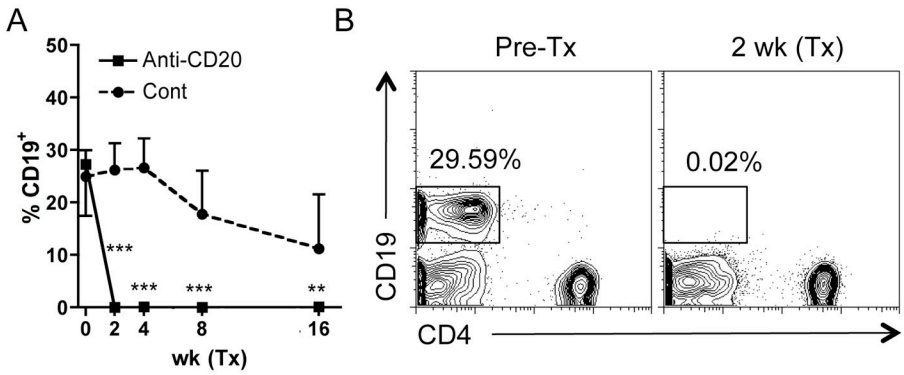

Figure 1.

Time course of peripheral frequency of $CD19^+$ cells in anti-CD20 treated dnTGF-βRII mice. A. Representative lymphocyte gated plots are shown for before and 2 weeks after anti-CD20 treatment. B. Administration of anti-CD20 mAb into peritoneal cavity from 4–6 weeks and 20–22 weeks of age efficiently deprived $CD19^+$ B cells from peripheral blood in dnTGF-βRII mice 2 weeks after initial treatment. Frequency of $CD19^+$ B cells was significantly lower in anti-CD20 treated dnTGF-βRII mice (n=7 and 7 in younger and older groups respectively) than controls (n=9 and 7). (***: $p < 0.001$ in Mann-Whitney Test in B.)

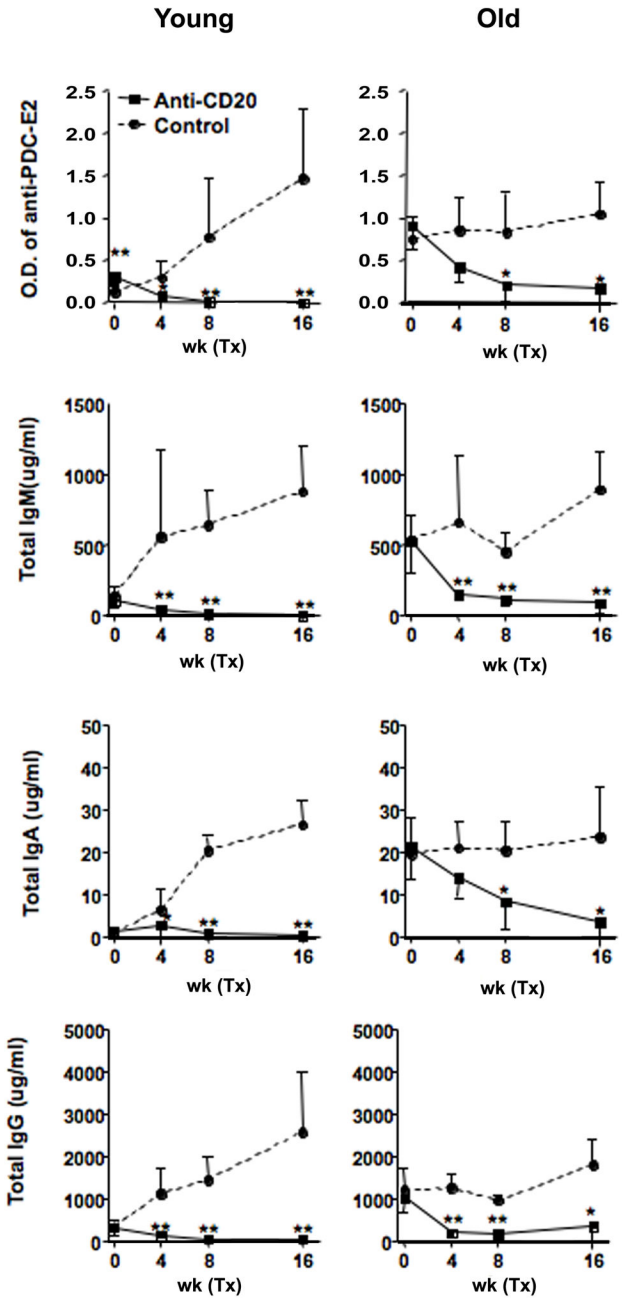

Figure 2.

Serum levels of anti-PDC-E2 and immunoglobulin in anti-CD20 treated dnTGF-βRII mice. Serum reactivity to PDC-E2 was significantly lower in anti-CD20 treated dnTGF-βRII mice (n=6 and 5 in younger and older groups respectively) than controls (n=6 and 5) 4 weeks after initial treatment whereas the reactivity was higher in mice assigned for B cell depletion in the younger group. Serum levels of IgM, IgA, IgG were also significantly reduced by anti-CD20 treatment. (*: $p < 0.05$, **: $p < 0.01$ in Mann-Whitney Test)

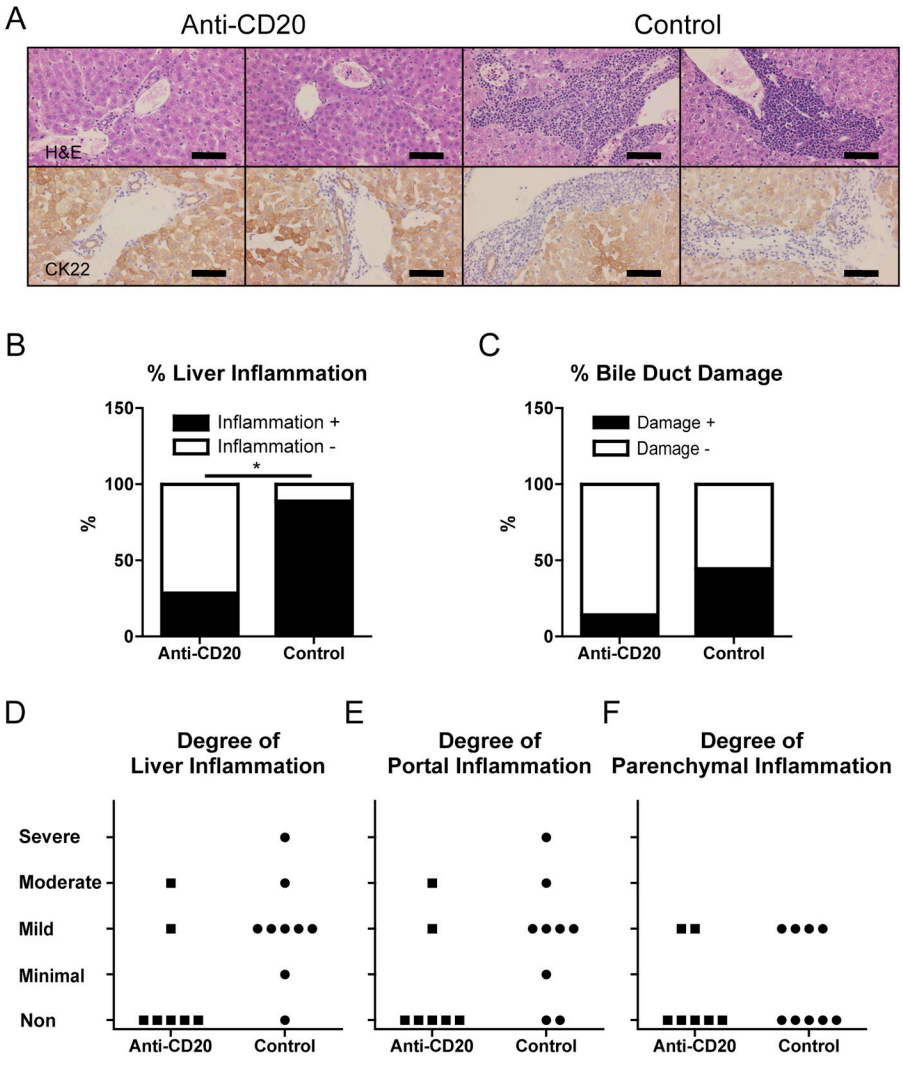

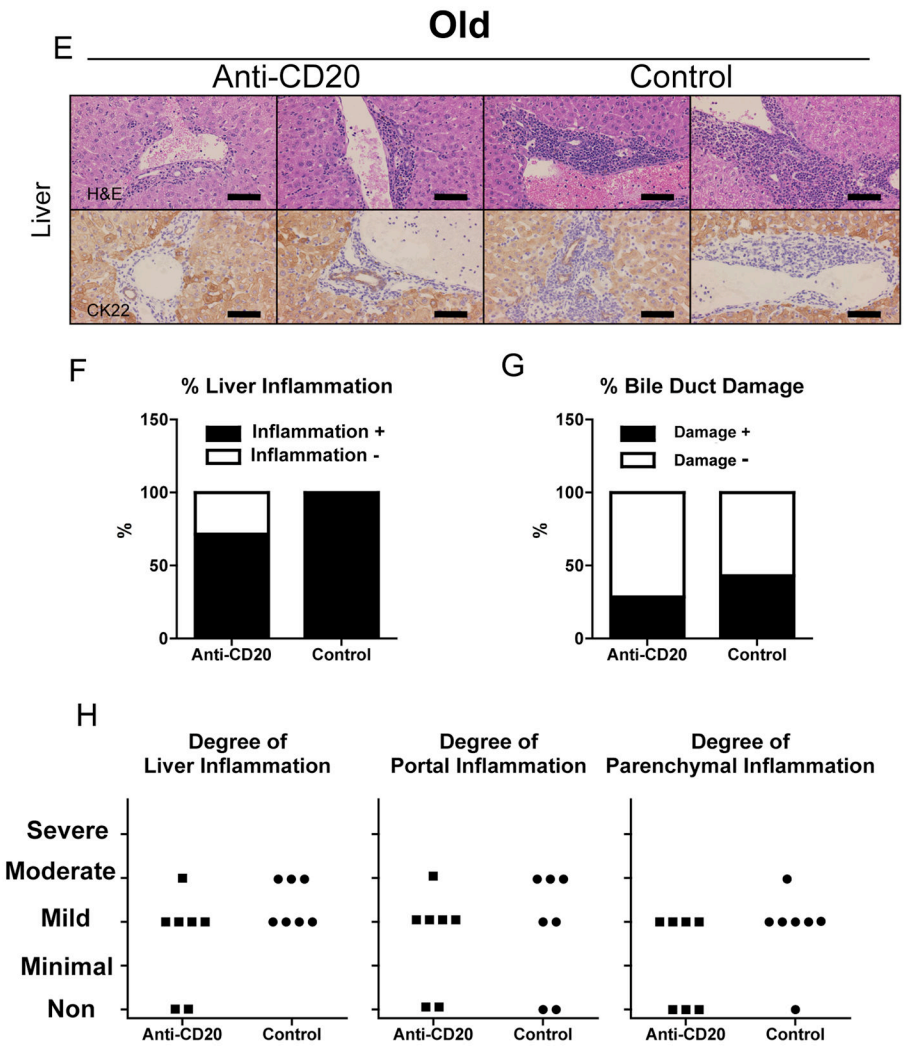

Figure 3.

PBC-like liver pathology was ameliorated in anti-CD20-mAb treated younger, but not older, dnTGF-βRII mice.

A. Liver sections at 20–22 weeks of age after 16 weeks treatment showing in anti-CD20-mAb treated dnTGF-βRII mice milder levels of cellular infiltrates around interlobular bile ducts than in control-mAb treated dnTGF-βRII mice. CK22 demonstrated damaged bile ducts in control dnTGF-βRII mice. B. Liver Inflammation was evaluated in each liver section. Frequency of liver inflammation-positive sections was significantly lower in anti-CD20-Ab (n = 7) treated dnTGF-βRII mice than control-mAb-treated mice (n = 9). C. Bile duct damage was also evaluated for each sample. D. Liver, portal, and parenchymal inflammation score was demonstrated for each sample in the younger group of mice. E. Some livers from anti-CD20 treated mice at 36–38 weeks of age after 16 weeks treatment demonstrated milder levels of cellular infiltrates than those of controls. CK22 demonstrated damaged bile ducts in anti-CD20-mAb treated older mice and controls. Bile duct paucity was demonstrated in a portal area of controls. F. Frequency of liver inflammation-positive sections did not differ significantly between anti-CD20 treated older dnTGF-βRII mice (n =

7) and controls (n = 7). G. Bile duct damage was not regulated by anti-CD20 treatment. H. Liver, portal, and parenchymal inflammation score was demonstrated for each sample in the older group mice. (H&E and CK22 staining. Black scale bars indicate 100 μm in A and E. *: $p < 0.05$ in Fisher's Exact Test)

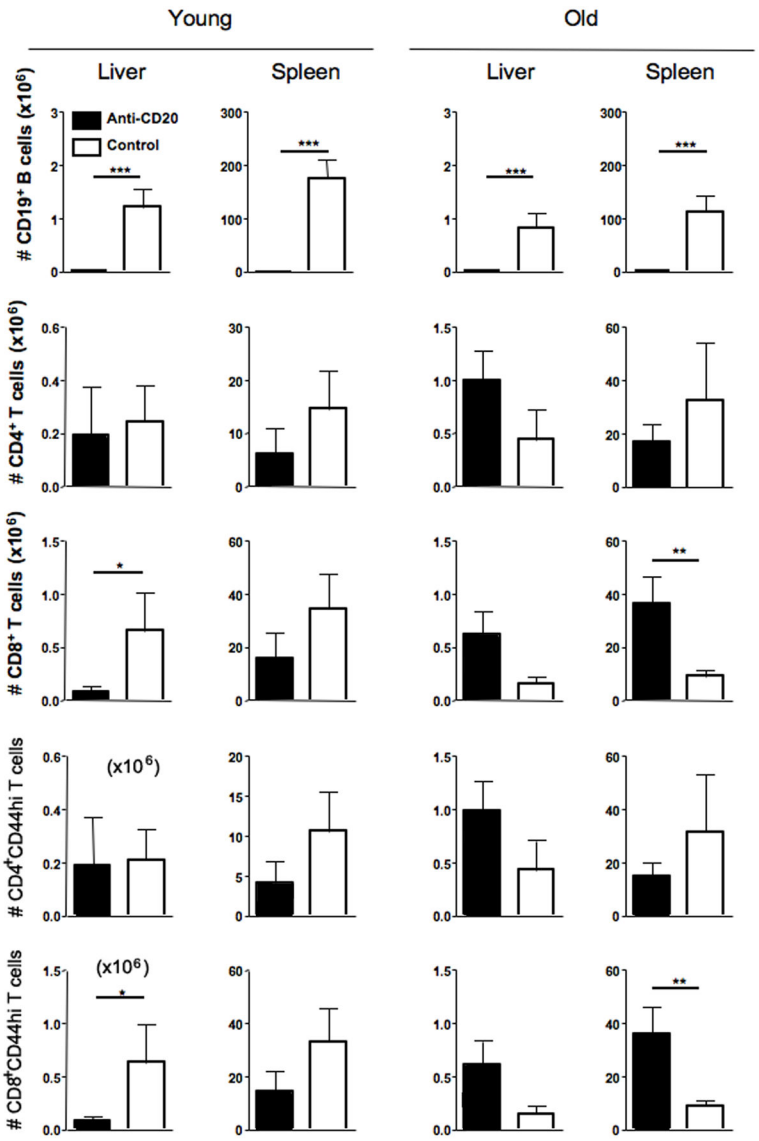

Figure 4.

Immunological profiles of liver MNC in anti-CD20-mAb- and control-mAb-treated dnTGF-βRII mice.

Absolute numbers of $CD19^+$ B, $CD4^+$ T, $CD8^+$ T, $CD44^{hi}CD4^+$ T, and $CD44^{hi}CD8^+$ T cells were demonstrated for gram of liver and spleen. Depletion of $CD19^+$ B cells was accomplished in both liver and spleen by anti-CD20 treatment in younger and older groups. Absolute number of liver $CD8^+$ T cells and their activated phenotypes were significantly decreased in livers of anti-CD20 treated younger dnTGF-βRII mice (n = 6) compared to that of control-mAb-treated mice (n = 8) whereas those difference was not obvious in older mice after anti-CD20 treatment. (*$p < 0.05$, **$p < 0.01$, ***$p < 0.001$ in Mann-Whitney Test)

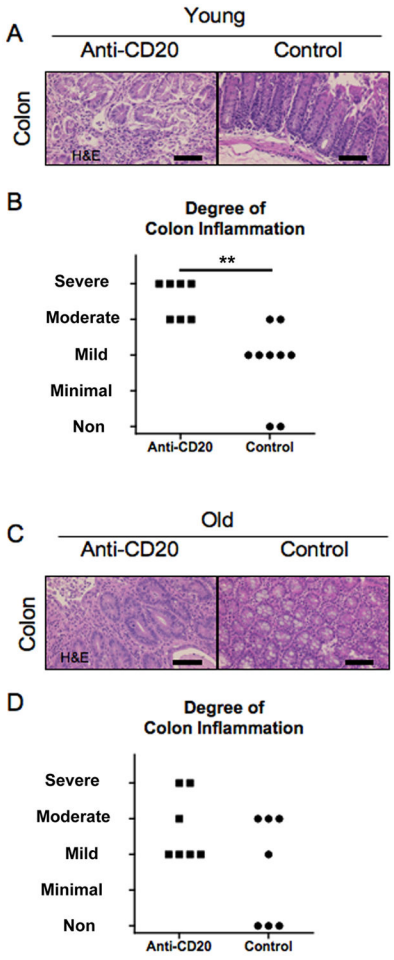

Figure 5.

Colitis was exacerbated in anti-CD20 treated younger dnTGF-βRII mice.

A. Sections of colon at 20–22 weeks of age after 16 week treatment showing severe inflammation in all layers in anti-CD20 treated dnTGF-βRII mice contrasting with mild inflammation in dnTGF-βRII mice. B. Degree of colon inflammation was significantly greater in anti-CD20 treated mice (n = 7) than control mice (n = 9). C. Some of anti-CD20 treated colon at 36–38 weeks of age after 16 week treatment demonstrated severer inflammation in anti-CD20-mAb-treated dnTGF-βRII mice contrasting with no inflammation in some of control-mAb treated colon, however, those did not differ significantly. (H&E staining. Scale bar 100 μm in A, **: $p < 0.01$ in Mann-Whitney Test)

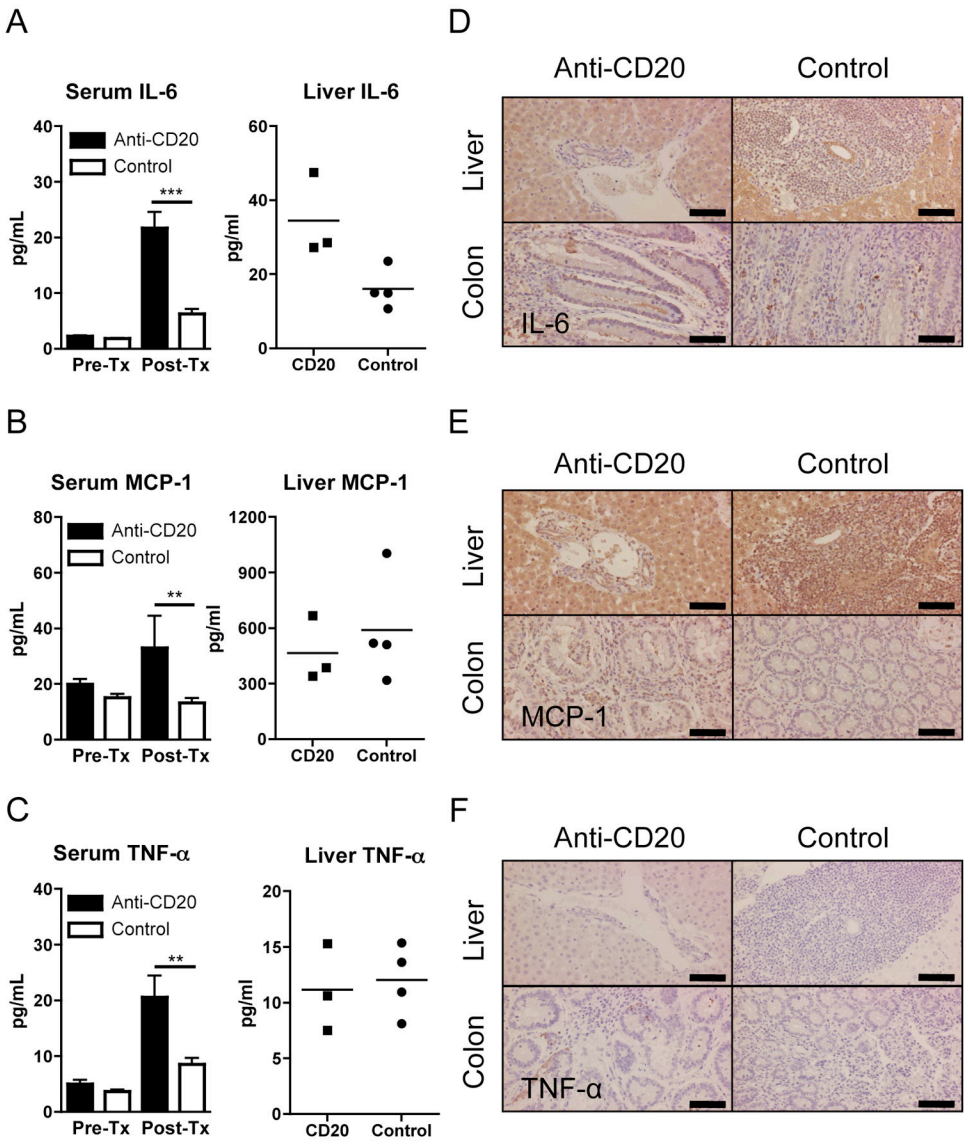

Figure 6.

Inflammatory cytokines in anti-CD20-treated younger dnTGF-βRII mice.

A–C. Mean serum cytokine levels in mice at 20–22 weeks of age after16 week treatment, using a cytometric bead array kit. IL-6, MCP-1, and TNF-α were significantly increased in anti-CD20 treated dnTGF-βRII mice (n=7) compared with control-Ab-treated dnTGF-βRII mice (n=9). Levels of IFN-γ, IL-12p70, and IL-10 were lower than detectable ranges in the serum samples from either strain (data not shown). Liver cytokines were also examined in anti-CD20 treated and control mice. Liver IL-6 was significantly higher in anti-CD20 treated mice (n=3) than controls (n=4), while MCP-1 was comparable and TNF-α was lower than detectable range. D–F. Immunohistochemical detection of IL-6, MCP-1 and TNF-α. IL-6 was detectable in hepatocytes and bile duct epithelial cells, but faint in mononuclear cells of liver. IL-6 positive mononuclear cells were scattered in colon of both groups while cytoplasm of epithelial cells and lumens of cryptae were IL-6 positive in anti-CD20 treated

mice. MCP-1 was detectable in Kupffer cells, mononuclear cells, and hepatocytes while slightly positive in bile duct epithelial cells in liver. MCP-1 was detected in mononuclear cells in colon. Frequency of MCP-1 positive cells was greater in colon of anti-CD20 treated mice. TNF-α staining demonstrated numerous positive mononuclear cells in colon, but not in liver, of anti-CD20-Ab-treated mice whereas no positive cells were observed in either colon or liver of control mice. (**: $p < 0.01$, ***: $p < 0.001$ in Mann-Whitney Test in A–C for sera. Scale bar 100 μm in D–F)